Flow Charts and Lubricated Transport of Foams

Travis A. Smieja, Daniel D. Joseph and Gordon Beavers

University of Minnesota

July 2001 *file: 2000/papers/LubTransport/foam.-*

Abstract

The flow characteristics of aqueous foams were studied in a thin flow channel instrumented for pressure gradient and flow rate measurement. The quality of the foam was varied by controling the volumetric flow rates of liquid and gas, and different flow types were identified and charted. Dry foams move as a rigid body lubricated by water at the wall. A simple lubrication model leading to an expression for the thickness of the lubricating water layer is presented.

1 Introduction

There are many applications for flowing foams. In the oil industry foams are used, for example, in under-balanced drilling, for reservoir cleanup and for enhanced oil recovery in porous sands. For these applications the flow characteristics depend on flow types which have not yet been charted in channel flow. The lubrication property of dry foams which is of special interest seems not to have been studied before.

2 Experiments

The foams used in these experiments were generated in a solution of 0.06% by weight of 98% dodecyl sulfate, sodium salt (SDS) plus 1.0% by weight of 1-butanol in de-ionized water. This concentration was selected based on the results

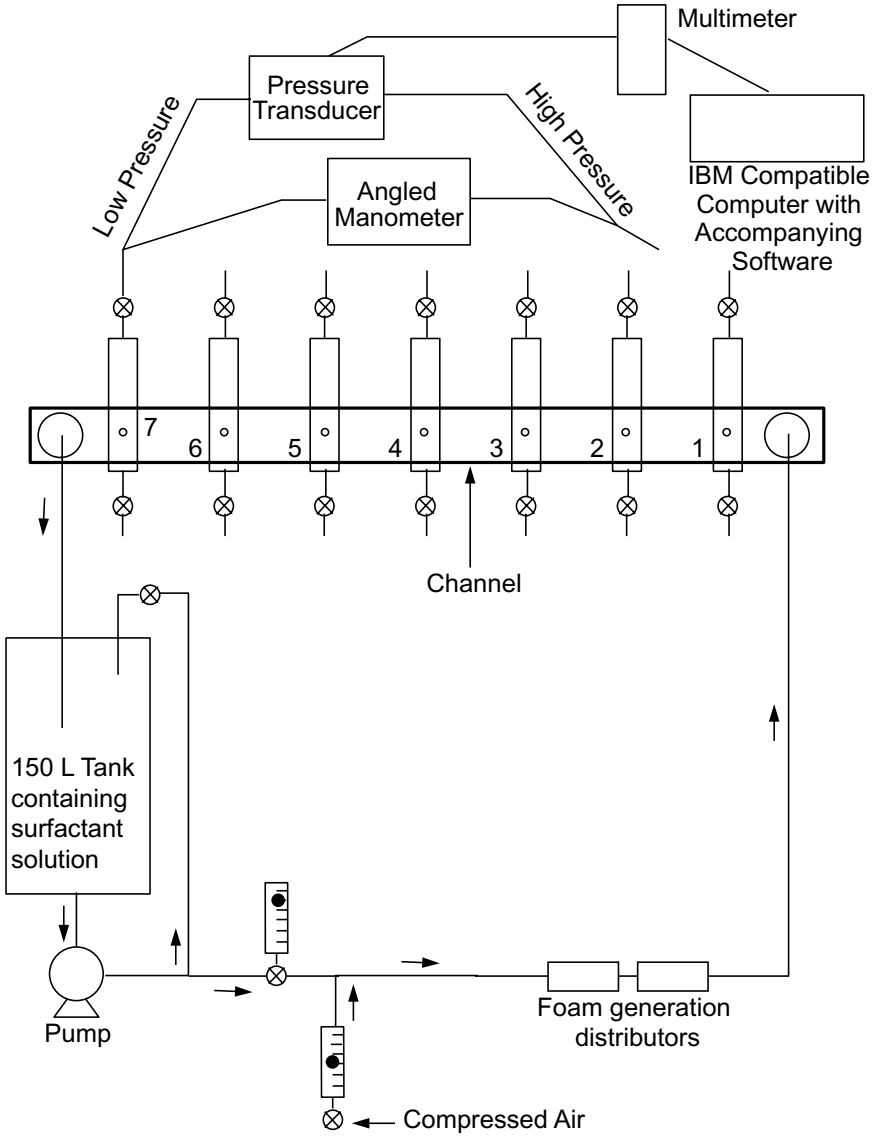

Figure 2.1: *Experimental setup for the measurements of pressure in foam flowing through a horizontal channel. The flow channel has a length of 43 in., a width of 1 in. and a depth of 1/4 in. There are seven taps connected to the channel and the differential pressure of any two taps is measured by both an angled manometer and a pressure transducer. The foam flows clockwise in the diagram from the pump to the channel and back into the 150-liter reservoir.*

of the experiments by Ling Jiang [1], which showed that this particular concentration produced a fine, stable foam. To ensure freshness of the surfactant, it was prepared within 24 hours of being used.

The flow loop is shown in Figure 2.1. The heart of the loop is a horizontal rectangular plexiglas channel, containing seven equally-spaced ports for local pressure measurements. Initially, 22.71 liters (six gallons) of the surfactant liquid were placed into the 150-liter (40-Gallon) tank. This large tank allowed ample room for the foam, upon returning from the flow channel, to break down to surfactant. A Dayton split phase pump motor (model $^{\#}$6K160C) with a TEEL vane pump attachment was used to pump the surfactant from the bottom of the tank. Upon leaving the pump the surfactant was split between two tubes, one of which was used as a bleeder (because the pump was a constant speed pump), while the other tube fed into a Gilmont $^{\#}$15 liquid flow meter. The surfactant was mixed with compressed air just downstream of the liquid flow meter through the use of a Y-junction. The compressed air first flowed through a Ohio Medical Products Airco Oxygen regulator (stock $^{\#}$9476) and a custom air damper to ensure smooth, steady airflow. Once through the Y-junction, the bubbly mixture was passed though two different distributors to enable the production of fine foams. The first distributor was a porous metal plate (pore size 125 μm). From there it passed into a 3/4 in. inner diameter Nalgen reinforced (175 WP) PVC tube, containing small glass beads ranging in size from 2360 microns to 2800 microns, where the glass beads acted as the second distributor. The foam then entered the horizontal channel.

The measurement of the local pressure at each of the seven locations was accomplished using special pressure taps. Each tap consisted of a vertical Plexiglas tube, 15 cm long and 1.2 cm diameter, bonded to the side of the channel with access to the channel pressure through a 2.0 mm diameter hole at the point of attachment. Access ports to the tubes were installed in the top and bottom ends, (Figure 2.2). Foam from the channel entered the tap, which was partially filled with de-ionized water to assist in the breaking up of foam in the tap, so that pressure measurements could be taken over a longer time. The water was loaded from the bottom port, which was closed when pressure measurements were being recorded.

Pressure gradients were constructed from pressure difference measurements between tap #7 (the tap closest to the channel exit) and each of the other 6 taps. Figure 2.2 shows two taps and the two systems used for measuring the pressure

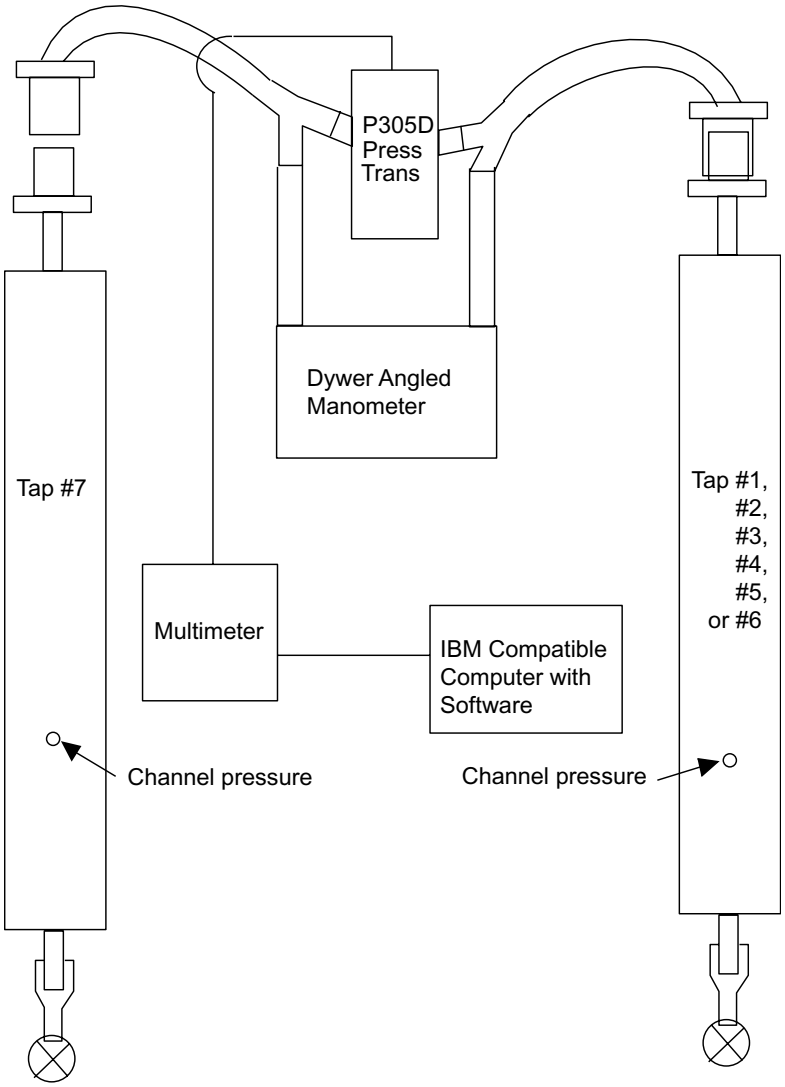

Figure 2.2: *Schematic diagram of how two taps connect to both pressure measurement devices.*

difference between them. Tubing connected the top of each pressure tap cylinder to a valve which was closed when the tap was not being used for a pressure measurement, and which connected the tube to a Y-junction when the tap was being utilized. The Y-junction allowed the pressure to be measured by devices. These were Dwyer Instruments Inc. angled manometer (range 0-23 in. H_2O) using specific gravity blue gage oil, and a Validyne pressure transducer (model $^{\#}$ P305D). An accurate reading of the pressure was difficult to obtain from the manometer because of constant fluctuations. The manometer was used simply as a rough check on the pressure transducer output. The pressure transducer was connected to an Extech Instruments Digital Multimeter (Model$^{\#}$383273), which came with appropriate PC interface software. The software allowed the P305D to record the measurements at different sample rates and then insert them into a spreadsheet program. The time-sampling rate was used to generate the average value of the pressure. All pressure measurements were recorded until almost the entire cylinder of the tap was filled up with foam, but stopped prior to foam entering the tube connected to the top of the cylinder.

3 Procedures

Before the start of an experimental run, the water levels in the seven taps were adjusted, all lines and taps were examined to establish that no foam or air bubbles were present, and all the valves on the pressure taps were closed. This was necessary so that no foam entered the taps before the desired steady state foam flow was reached.

It was found that the most efficient way to investigate different combinations of air and liquid flow was to fix the liquid flow rate, while systematically stepping through the range of gas flow rates. For each gas flow rate, a steady state was achieved by keeping the flow rates of both the gas and liquid constant for at least five minutes prior to measuring the pressure. The following ranges of flow rates were used: liquid 0.05, 0.1 and 0.2 L/min; gas 0.19 to 1.4 L/min with increments of approximately 0.2 L/min. After completing all the gas flow rate increments, the liquid flow rate was increased one step and then held fixed, while all the gas flow rates were stepped through again. This process was repeated for the third liquid flow rate. After finishing all the flow rate ranges for both liquid and gas, several sample combinations were repeated to check the earlier results.

After letting the flow reach steady state by retaining the desired flow rate values for at least five minutes, the sixth and seventh taps were connected to the Y-junctions linking the two pressure measurement devices. Then the valves to the sixth and seventh taps were opened, allowing the foam to start entering the taps thereby transmitting the local channel pressure to the recording devices. As the test was being conducted, the manometer was watched to estimate the average pressure. As soon as the sixth tap was almost completely filled with foam, the software on the computer was stopped, and both valves on the taps were closed. The tubing from the sixth tap was moved to the fifth tap and the above process was repeated. This was repeated until the pressure differences of the first six taps relative to the seventh tap were recorded. After letting the foam in the taps collapse, the process was repeated for a different set of flow rates.

4 Flow types for foam

B. Bunner [3] has identified four flow types: bubble flow, slug or plug flow, churn flow and annular flow. We encountered the first three types in our experiments.

They are illustrated in the photographs of Figures 4.1, 4.2 and 4.3, which show flow in a slip-type vertical channel. Figure 4.1 shows churn flow which according to Bunner consists of coarse, wet foam with large gas bubbles rotating and churning in a wet foam. The flow called bubble flow by Bunner could be called dry foam flow; it is composed of liquid films joined at plateau borders and it flows as a rigid body as shown in Figure 4.2. In slug flow, shown in Figure 4.3, relatively large gas bubbles appear interspersed in the foam. However, in our experiment the air bubbles are much smaller because of the glass beads in the tubing used to break up large air bubbles prior to entering the channel. Finally, for annular flow the foam is collected to the side walls of the channel, while the center is filled by a rapid gas flow. Unfortunately the range of gas flow rates used for this experiment was not large enough to make this happen because the flow meter only allowed a maximum gas volumnetric flow rate of 2.3 L/min, less than needed for annular flow.

Perhaps the chief difference between flows with large bubbles and dry foam (small bubbles) flow is that the large bubbles move relative to the surrounding flow.

The construction of our flow type Table 4.1 was based on visual identification of flow types, which was facilitated by our slit-type of flow channel. At low gas flow rates the flow starts as churn flow. As the gas flow is increased the flow evolves first to bubble or dry foam flow; then as the gas flow is increased past the point that the dry foam can transport the injected gas, slug flow develops, which transports the gas faster than the surrounding foam. If the gas flow rate could be increased even more, the foam flow characteristic would then turn into annular flow, based on the results of Bunner.

One of the major reasons that the oil industry is interested in foams is to transport particles, as in forcing the oil-well drill cuttings up and out of the well. From the visual analysis of the foams flowing in the vertical channel it appears that only the bubble flow characteristic would be able to transport particles up a well. This is because it is the only flow regime in which the foam in the entire channel moves as a rigid body. Another reason it would be a good transporter of particles is because the entire rigid body foam consists of fine bubbles that would likely be able to trap particles in between them as the rigid foam flow would transport the particles up the well. The churn flow appears to contain too much liquid to adequately transport particles, since the majority of the drill cuttings are more dense than the liquid and thus they would sink. While the slug flow contains some fine bubbles

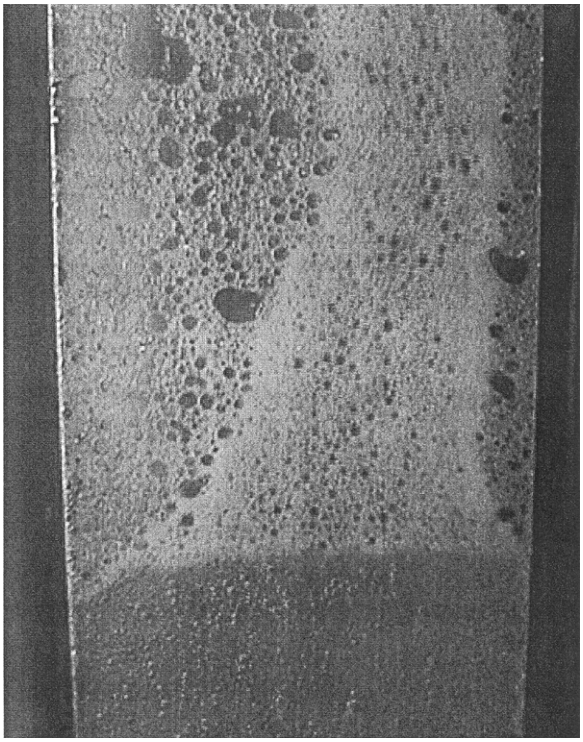

Figure 4.1: *Churn flow in a vertical channel. Note that the churn flow in this channel contains much smaller air bubbles because of the small glass beads in the entrance tube which prevent large air bubbles from entering the channel. However, this flow type consists of a very wet foam with air bubbles rising rapidly through it.*

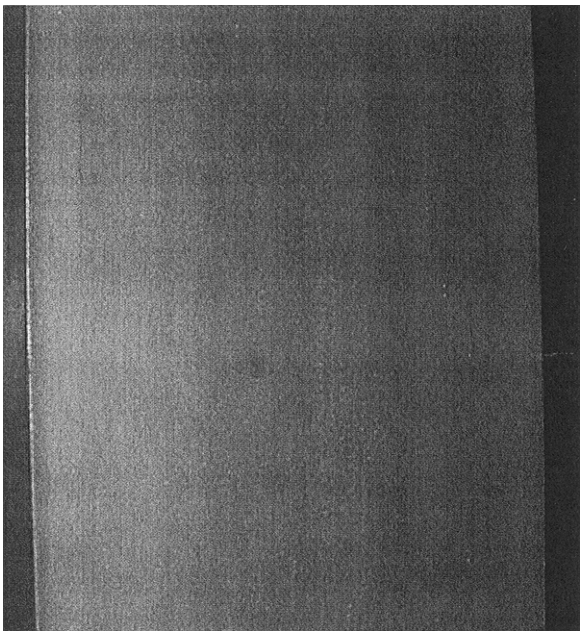

Figure 4.2: *Bubble flow in a vertical channel. As this figure illustrates the bubble flow classification consists of the entire channel being filled with a fine foam, flowing as a rigid body.*

to trap the particles, the large rapidly-moving slugs generally break these smaller bubbles, which would then release the trapped particles. Thus it is believed that the only foam flow characteristic that could adequately transport particles is bubble flow.

5 Pressure measurements

In Figures 5.1, 5.2 and 5.3 we have reported the pressure readings at the taps shown in Figure 2.1 (relative to tap #7) for different gas rates at a given liquid flow rate. There is no data point for tap number 4 because a small leak in the top of the tap caused significant discrepancies in the pressure readings. In Figure 5.1 the first tap (greatest tap separation distance) has been omitted for the lightest gas flow rate, because the foam filled the tap too rapidly to get an accurate average of the pressure difference between it and the seventh tap.

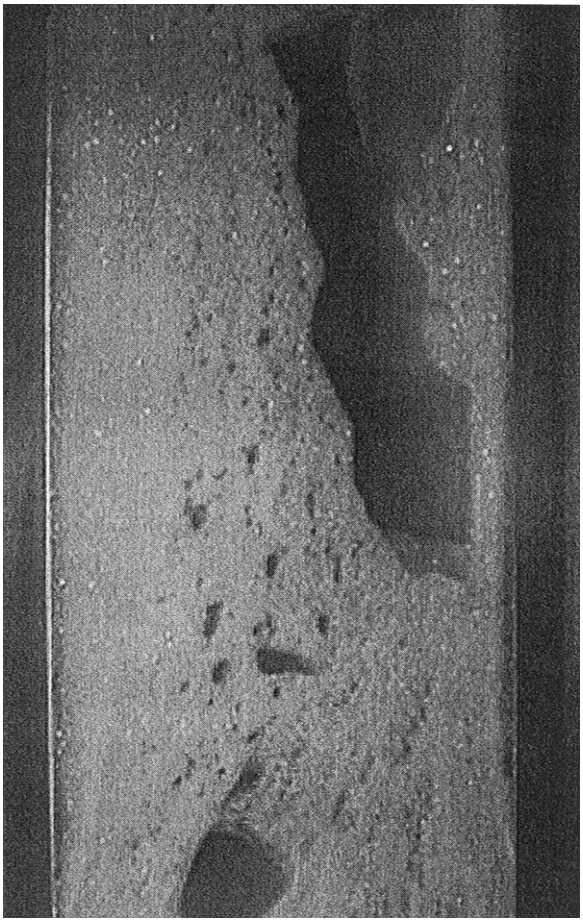

Figure 4.3: *Slug or plug flow in a vertical channel. This flow classification consists of large air bubbles (slugs or plugs) traveling along the center of the channel surrounded by foam and possibly a few smaller air bubbles.*

Q_l (L/min)	Q_g (L/min)	Foam Regime Classification Table													
	0.19	0.40	0.59	0.76	0.93	1.09	1.24	1.39	1.54	1.67	1.81	1.93	2.05	2.17	2.31
0.05	C	TB	B	B	B	TS	S	S	S	S	S	S	S	S	S
0.10	C	TB	B	B	B	B	B	B	B	B	B	TS	S	S	S
0.20	C	C	TB	B	B	B	B	B	B	B	B	B	B	B	B

Table 4.1: *Table listing all the visual foam flow characterestics observed in this experiment.* C *denotes churn flow,* B *denotes bubble flow,* S *denotes slug flow and a* T *immediately proceeding any of these letters indicates that it was in transition from the cell before it, to the foam flow type next to the letter* T.

Figure 5.1 shows the pressure distribution for a liquid flow rate of 0.05 L/min and a range of gas flow rates from 0.19 to 1.0 L/min. The trend lines for the pressure are nearly linear; the average of all the lines R^2 values is 0.991, meaning on average the data points are within one percent of being perfectly linear. Another observation from this first figure is that as the gas flow rate is increased for a fixed liquid flow rate, the slope of the pressure distribution line also increases. Therefore, as the foam becomes drier (increased gas flow rate while maintaining a constant liquid flow rate) the pressure drop along the channel increases.

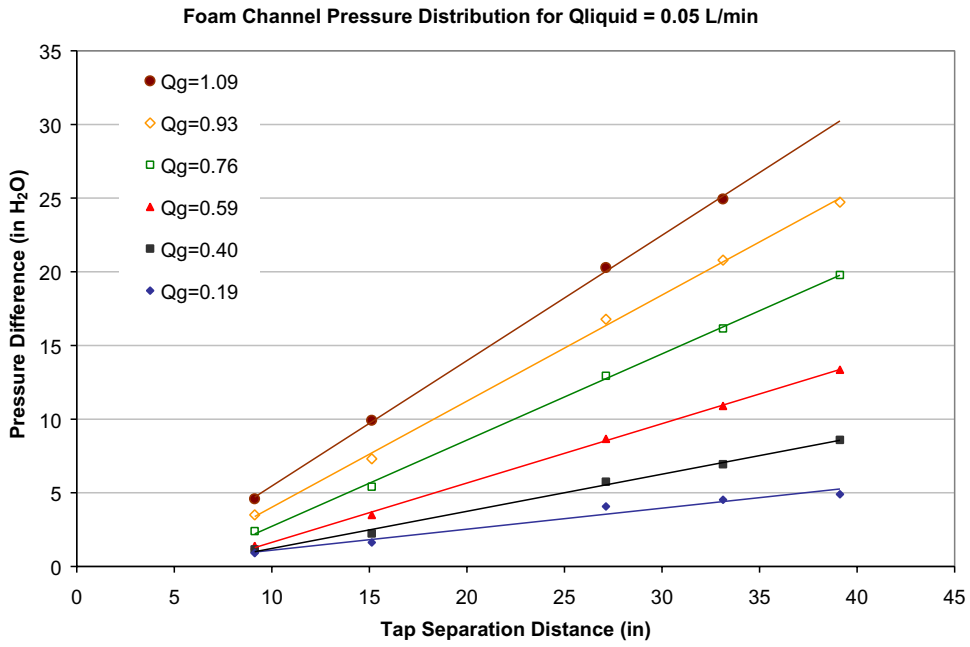

Figure 5.1: *Plot of the pressure distribution through a horizontal channel for a liquid flow rate of 0.05 L/min and a range of gas flow rates from 0.19 L/min to 1.0 L/min. This figure illustrates that the pressure distributions are nearly linear. As the gas flow rate increases, so does the pressure drop, implying that drier foams produce greater pressure drops across the channel.*

Figure 5.2 shows the pressure distribution for a liquid flow rate of 0.1 L/min and a range of gas flow rates from 0.19 to 1.24 L/min. The reason the gas flow rate range was greater for these tests was because it was a wetter, slower moving foam so the taps did not fill up as rapidly, allowing sufficient time to obtain an average pressure reading at higher gas flow rates. The same general statements about Figure 5.1 can also be made about this figure: the pressure distributions are linear in nature and an increasing gas flow rate (i.e. drier foam) leads to a larger pressure drop across the channel.

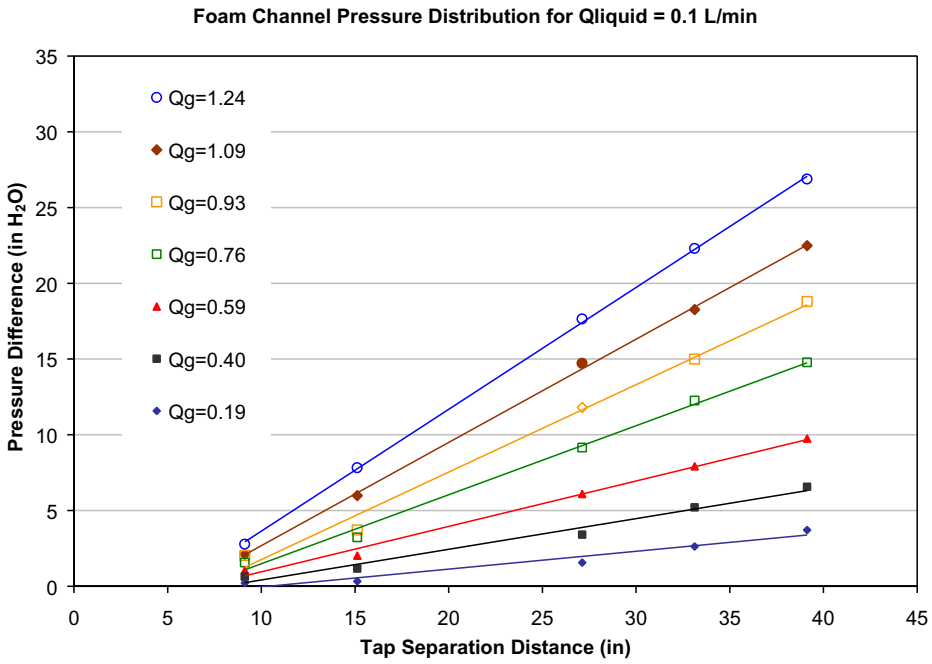

Figure 5.2: *Plot of the pressure distribution through a horizontal channel for a liquid flow rate of 0.1 L/min and a range of gas flow rates from 0.19 L/min to 1.24 L/min. This figure shows that the pressure distributions are linear in nature and a drier foam produces a larger pressure drop across the channel.*

Figure 5.3 shows the pressure distribution for a liquid flow rate of 0.2 L/min and a range of gas flow rates from 0.19 to 1.4 L/min. The same general statements about the previous two figures can also be made about this figure: the pressure distributions are linear in nature and an increasing gas flow rate leads to a larger pressure drop across the channel.

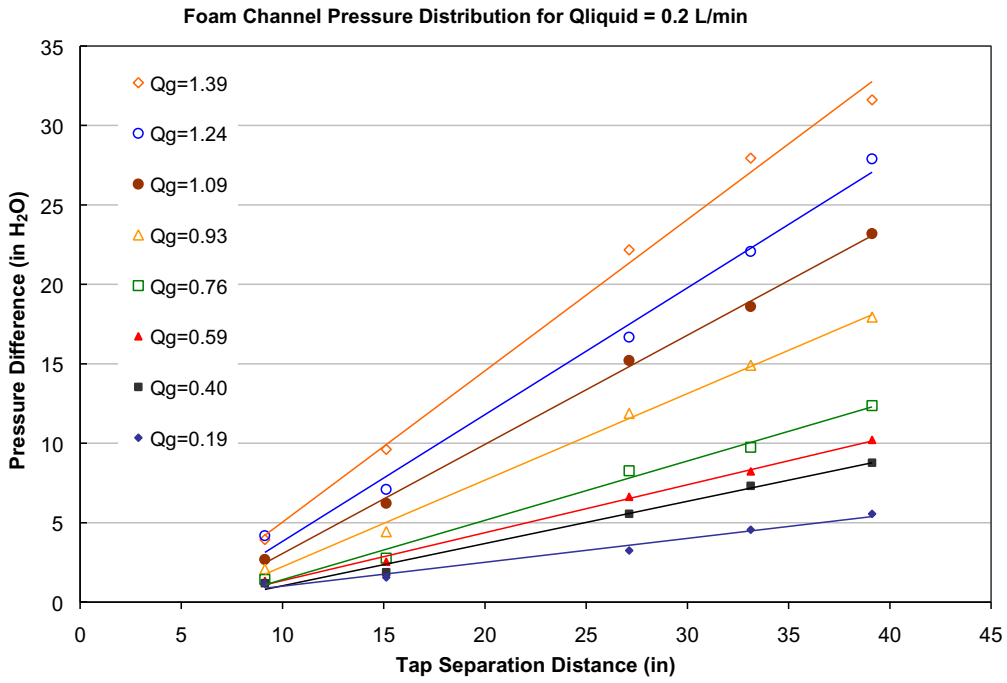

Figure 5.3: *Plot of the pressure distribution through a horizontal channel for a liquid flow rate of 0.2 L/min and a range of gas flow rates from 0.19 L/min to 1.4 L/min. As expected the pressure distributions are linear in nature and as the gas flow rate was increased, the pressure drop across the channel also increased.*

6 Lubrication of dry foams

Dry foam, called bubbles in the Bunner classification, moves as a rigid body with trapped gas in lock step with liquid films trapping gas. Since there is almost no relative motion of gas and liquid we could say that the dry foam has a surprisingly high viscosity. How does it flow? The rigid foam slides on a lubricating layer of water. The frictional resistance to the flow of gas is provided by the shear stress in the water layer which in our experiments appears to be in a laminar Couette flow, decreasing linearly to zero from the value of the velocity of the rigid core.

We can identify the inception of the lubricating layer from the pressure gradi-

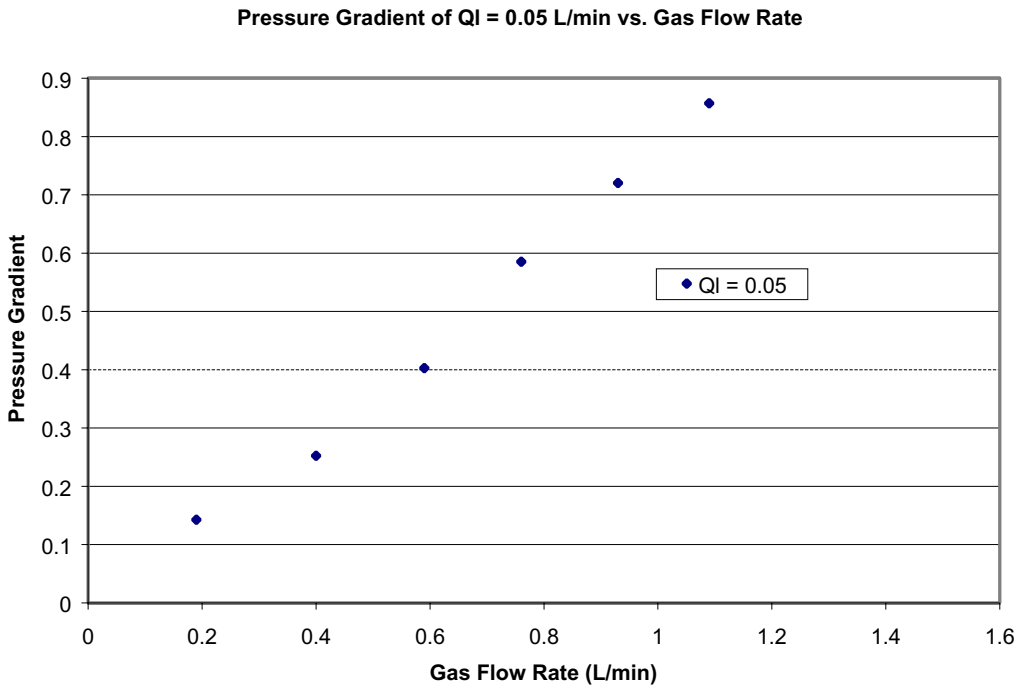

Figure 6.1: *Pressure gradient vs. gas flow rate for a liquid flow of 0.05 L/min. The upper portion is basically linear indicating lubrication.*

ent plots 6.1, 6.2 and 6.3 obtained as the slop of the lines shown in Figures 5.1– 5.3. In our diagram of lubrication the pressure gradient vs. gas flow at a given liquid flow rate is strictly linear, and a strictly linear region emerges at high gas flow rates in each of the cases.

The smaller the thickness of the lubricating layer δ, for a given gas velocity, the greater is the shear stress on the channel walls. Since the integral of the shear stress on the channel walls balance the pressure gradient force, the pressure gradient should be a decreasing function of the layer thickness δ. Though we have no direct measurements of the layer thickness we may suppose that it correlates with the water flow rate Q_l with higher pressure for lower values of Q_l, as shown in figure 6.4.

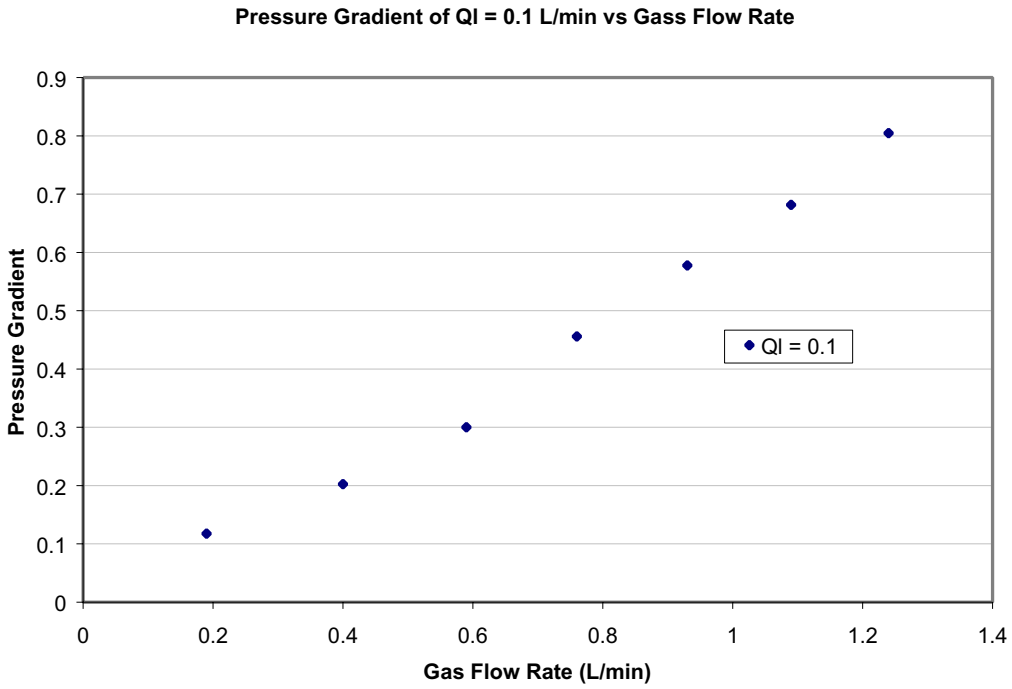

Figure 6.2: *Pressure gradient vs. gas flow rate for a liquid flow of 0.1 L/min.*

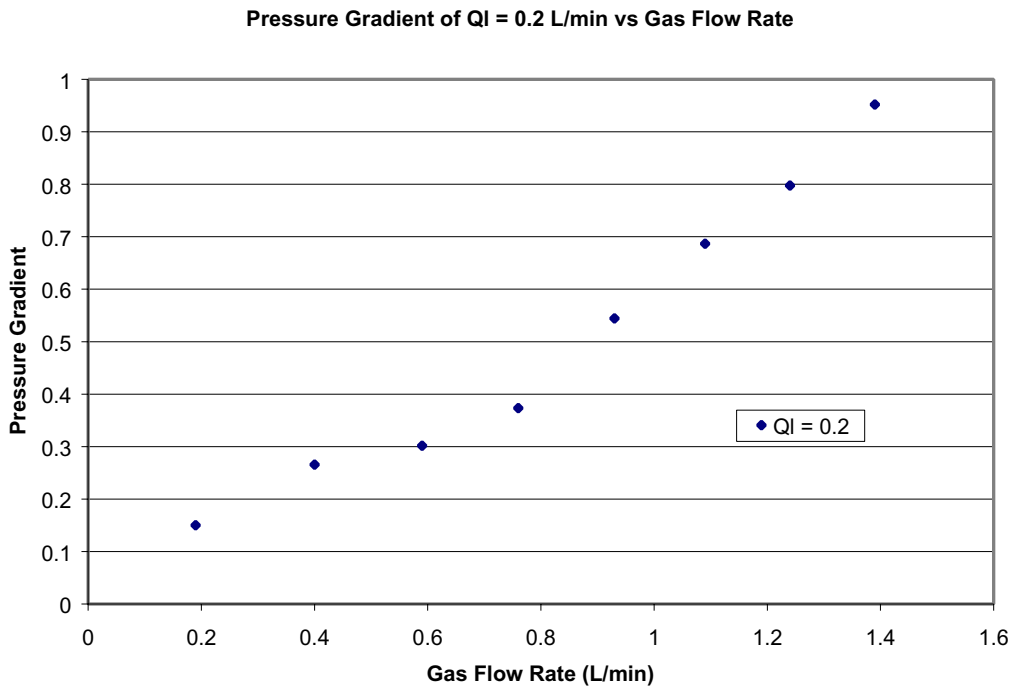

Figure 6.3: *Pressure gradient vs. gas flow rate for a liquid flow of 0.2 L/min. There is an abrupt change to lubrication at a gas flow of about 0.8 L/min.*

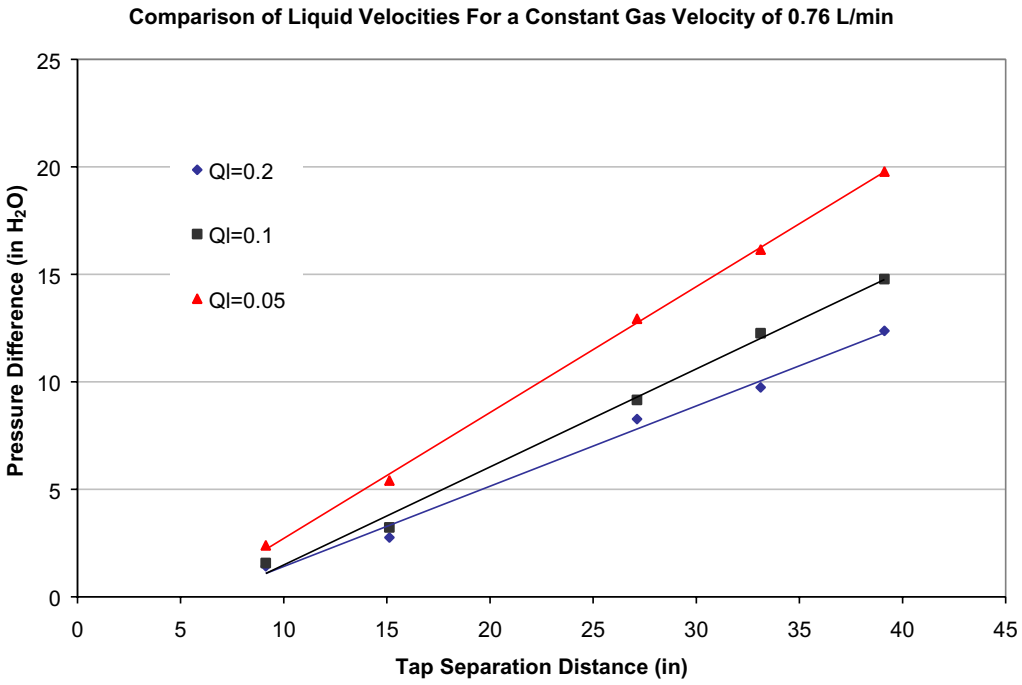

Figure 6.4: *Plot of the pressure distribution through a horizontal channel for a gas flow rate of 0.76 L/min and a range of liquid flow rates (0.05, 0.1 and 0.2 L/min). This figure illustrates that as the foam becomes drier, decreasing liquid flow rate for a fixed gas flow rate, the pressure gradient across the channel increases and that these pressure gradients appear linear in nature.*

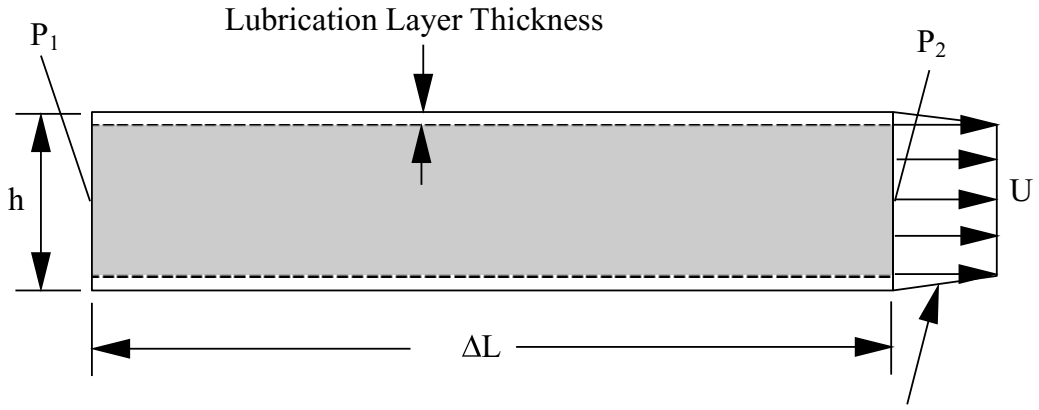

Figure 7.1: *Free body diagram of the foam flowing in a section of channel. The shaded region is the foam, traveling through the channel with a velocity U. The dimensions of the channel section are ΔL (the length), b (width), and h (height). There is a thin lubrication layer (thickness δ), since the foam is traveling as a rigid body.*

7 Lubrication model for flow of foams

Since the foam moves through the channel in a slug flow there is a small lubrication layer of thickness δ at the walls (Figure 7.1). A simple force balance equation was used to calculate δ as shown in Equation 7.1.

$$\Delta PA = (P_1 - P_2)A = 2(h + b)\tau\Delta L \tag{7.1}$$

where A is the channel cross-sectional area $\Delta P = P_1 - P_2$ is the pressure difference measured across a length of ΔL of the channel, b and h are the width and height of the channel, and τ is the wall shear stress.

Since this is a first approximation and the foam traveled as a rigid body (as illustrated in Figure 7.2) a linear approximation was made for the wall shear stress.

$$\tau = \mu\frac{dU}{dy} \approx \mu\frac{U}{\delta} \tag{7.2}$$

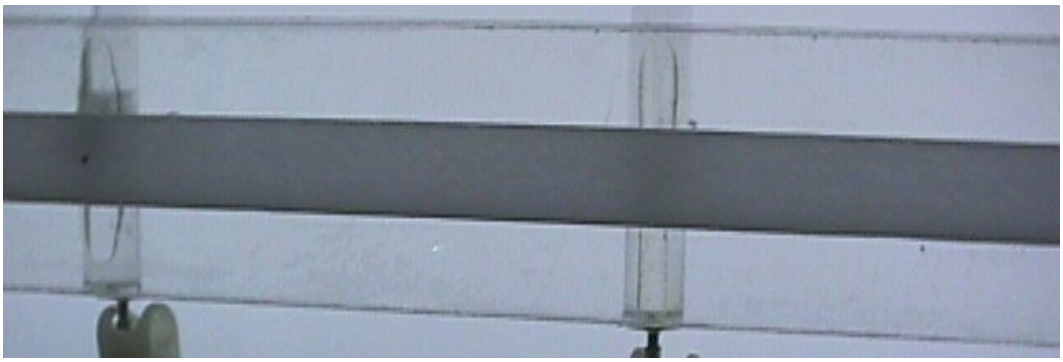

Figure 7.2: *Digital image of the foam flowing through the channel with a liquid volumetric flow rate of 0.05 L/min and a gas flow rate of 0.57 L/min. This image illustrates that the foam traveled as a rigid body, with a small lubrication layer surrounding the foam (dark lines on the top and bottom of the channel).*

Assuming that the lubricating layer is water (viscosity μ_w), and writing dP/dx for $\Delta P/\Delta L$, equations 7.1 and 7.2 give

$$\delta = \frac{2(h+b)\mu_w U}{A\frac{dP}{dx}} \tag{7.3}$$

The lubrication layer thickness was calculated using 7.3 and is plotted versus the pressure gradient along the channel in Figure 7.3, which shows that as the liquid flow rate increases for constant gas flow rates, the lubrication layer grows larger. This supports our belief that water is used as the lubrication to the foam, since as the liquid flow rate is increased at a fixed gas flow rate, the pressure across the entire channel decreases (Figure 6.4), and the lubrication layer increases.

This figure also illustrates that as the gas flow rate increases for a fixed liquid flow rate (going from left to right in Figure 7.3), the lubrication layer decreases as the gas flow rate is increased.

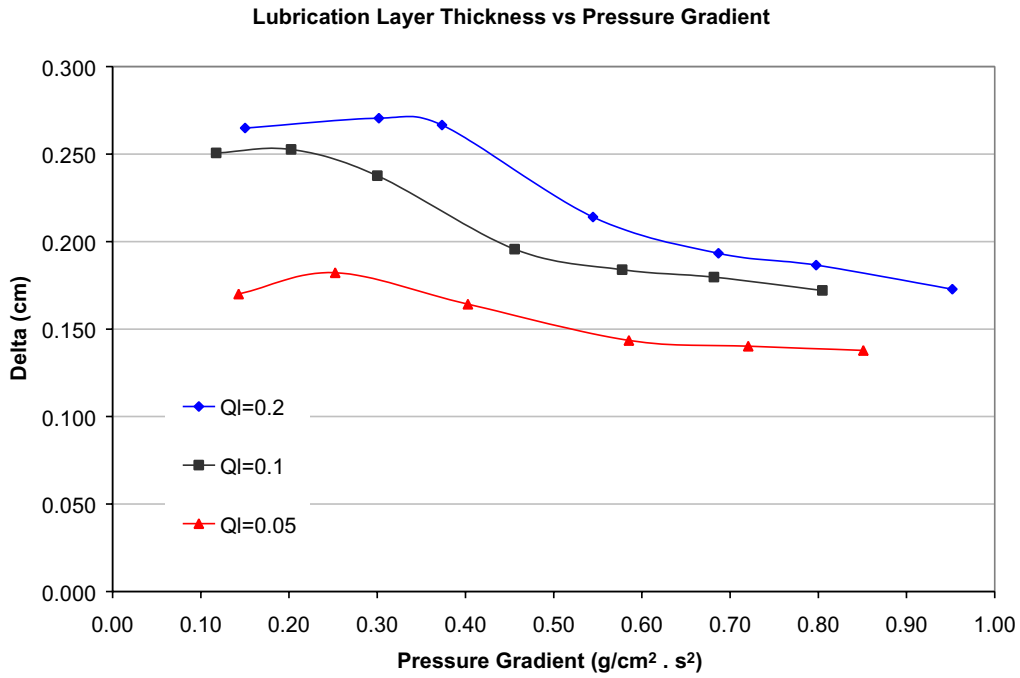

Figure 7.3: *Plot of the lubrication layer thickness versus the pressure gradient driving the flow. This graph illustrates that as the liquid flow rate is increased for a fixed gas flow rate, the lubrication layer thickness also increases, and as the gas flow rate is increased for a fixed liquid flow rate (moving from left to right on the plot) the lubrication layer thickness remains essentially unchanged at the lowest gas flow rates and then decreases with increasing gas flow rate.*

The data of Figure 7.3 were supported by qualitative examination of the flow. A flow was classified as lubricated if a liquid layer, or the effects of one, could be seen across the top or bottom of the channel. These observations are summarized in Table 7.1 This chart illustrates that as the liquid flow rate is increased a higher gas flow rate may still be lubricated, as shown by the gas flow rate of 1.24 L/min not being lubricated with a liquid flow rate of 0.1 L/min, but lubrication does occurs with a liquid flow rate of 0.2 L/min.

Liquid (L/min)	Gas Flow Rates (L/min) that are Lubricated
Q_L = 0.05	0.19–0.09
Q_L = 0.1	0.19–0.09
Q_L = 0.2	0.19–0.24

Table 7.1: *Lubrication chart indicating the visual lubrication inspection results during testing.*

8 Conclusions

The pressure distribution across a horizontal channel increases if the volumetric gas flow rate increases at a fixed liquid flow rate. As the ratio of the volumetric gas flow rate to the liquid flow rate is increased the lubrication layer thickness decreases. Thus, drier foams produce a greater pressure gradient and smaller lubrication layer thickness than wetter foams.

Acknowlegements. This work was supported by the Division of Engineering, Office of Basic Energy Sciences DOE, and by NSF/CTS under a GOALI grant in cooperation with Intevep S.A.

References

[1] Ling Jiang, November 1998, Masters Thesis, *Fluidization of Particles by a Gas Stream Through a Batch Particle/Liquid Suspension in a Tubular Bubble Column,* University of Minnesota.

[2] Tsutsumi, Dastidar and Fan, June 1991. Characteristics of gas-liquid-solid fluidization with non-wettable particles, *AIChE Journal*, **37**, 951-952.

[3] Bernard Bunner, 1997. Simulation of Large Bubble System, *Advances in Numerical Modeling of Free Surface and Interface Fluid Dynamics*, **9**.